

OVERVIEW OF THE RADIANT TIME SERIES METHOD

Calculation Procedure

The radiant time series method (RTSM) is a two-stage procedure for cooling load calculations (Spitler et al. 1997). First, hourly heat gains in a designated building space are calculated or estimated. The heat gains may include internal gains from lights, equipment, or human activity, conduction through the building envelope, convection from infiltration and ventilation, and transmitted and absorbed solar heat gains. Fixed fractions are used to split each internal heat gain into a radiative and a convective component. Conductive heat gains are split according to the relative magnitude of the radiation and convection film resistances, as shown in Equation 1.

$$f_r = \frac{R_c}{R_r + R_c} \quad (1a)$$

$$f_c = 1 - f_r \quad (1b)$$

where

f_r = radiative fraction of conductive heat gain

f_c = convective fraction of conductive heat gain

R_r = radiation film resistance, (ft²·°F·h)/Btu ([m²·°C]/W)

R_c = convection film resistance, (ft²·°F·h)/Btu ([m²·°C]/W)

The RTSM does not use detailed surface heat balances to model the effects of convection and radiation. Instead, it estimates their combined effect on exterior surfaces using the sol-air temperature and relies on the second stage of the two-step procedure to handle the inside surface radiant exchange. Conductive heat transfer is therefore calculated from the sol-air temperature to the inside air temperature using the following periodic response factors (PRFs) formulation:

$$q''_{\theta} = \sum_{j=0}^{23} Y_{pj}(t_{e,\theta-j\delta} - t_{rc}) \quad (2)$$

where

q'' = heat flux for the current hour, Btu/(h·ft²) (W/m²)

Y_p = air-to-air periodic response factors, Btu/(h·ft²·°F) (W/[m²·°C])

t_e = sol-air temperature, °F (°C)

t_{rc} = constant room temperature, °F (°C)

θ = current hour; δ = time step

The air-to-air PRFs are response factors for a one-dimensional, transient conduction problem with a steady periodic driving force. PRFs directly scale the contribution of previous fluxes (in the form of temperature gradients) to the current conductive heat flux, as shown in Equation 2. As a result, the PRF series represents the transient thermal response of a wall.

The second-stage calculation procedure converts the hourly heat gains into cooling loads. The radiative heat gains are multiplied by the radiant time factors (RTFs) to obtain cooling loads. The RTF represents the response of the building space to a radiant pulse, and it is therefore dependent on the material properties of the building elements. On the other hand, the convective heat gains are independent of the building materials and represent instantaneous cooling loads. The total hourly cooling loads are the summation of the hourly radiative and convective values.

Assumptions

Since the RTSM is a heat balance-based procedure, the heat balance method (HBM) assumptions (Chantrasrisalai et al. 2003) equally apply to the RTSM. In addition, the following assumptions apply (McQuiston et al. 2000):

- All external and internal driving forces are steady-periodic, and the zone air temperature is constant.
- The outside and inside heat transfer coefficients are time-invariant and include the combined effect of convection and radiation.
- Solar transmitted beam radiation is distributed on the floor only, while other shortwave and longwave radiation is distributed uniformly on each surface in the building space. In the Toolkit version of the RTSM, reflected radiation also remains in the space.

Overprediction of Peak Cooling Loads By the RTSM

Rees suggested that the adiabatic zone assumption, which is implicit in the generation of the radiant time series, coupled with the “air-to-air” conduction calculation (Rees et al. 1998) is responsible for differences between the RTSM and the heat balance method. Applying the heat balance method to an adiabatic zone generates the radiant time series. Heat gains, once accounted for in the space, cannot be lost by either “surface-to-surface” conduction or radiation from the space. Overprediction of the cooling load occurs when radiation on the interior surfaces of the zone raise the inside surface temperature of a lightweight, conductive surface, such as a single pane of glazing, above the outside surface temperature. In this case, two types of heat transfer immediately follow. First, the elevation of the inside surface temperature increases the rate of inside convection and, as a result, increases the cooling load. This phenomenon is modeled by the air-to-air conduction calculation in the RTSM. Second, the change in surface temperature could cause surface-to-surface conductive heat loss. As shown in Figure 1, the sol-air to inside air temperature gradient ($T_3 - T_4$) is in the opposite direction of the inside surface to outside surface temperature gradient ($T_1 - T_2$). Under these conditions, the heat balance, which is based on the surface temperature gradient, predicts a heat loss, while the RTSM, which is based on the air temperature gradient, predicts a heat gain.

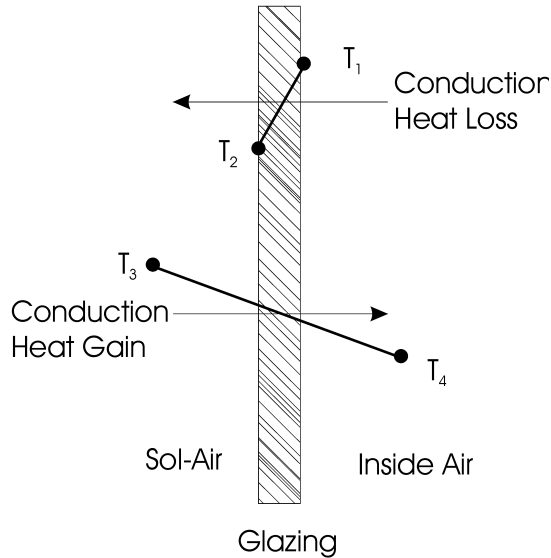


Figure 1 Opposing temperature gradients predicted by HBM and RTSM.

Unaccounted for conduction losses occur during periods of high solar heat gains when interior surface temperatures rise to create a surface temperature gradient that is not predicted by the RTSM. Rees et al. (1998) found that although the RTSM would never underpredict the space loads, it could overpredict the peak cooling load by as much as 37% for cases with a high percentage of glazing and low internal heat gains.

Figure 2, which compares the heat balance and RTS methods, shows essential agreement between the methods for a lightweight zone with 90% glazing. The agreement was achieved by eliminating the two known sources of error discussed in the previous paragraphs. First, for purposes of illustration, the thermal resistance of the window was increased to eliminate conduction that the RTSM does not account for. Second, reflected solar radiation losses through the windows were calculated. These two modifications result in excellent agreement between the methods for all zone configurations. The reflected radiation correction, though not included in the ASHRAE Loads Toolkit, can easily be added to future versions of the method.

Some error may also be made by assuming that surface convection and radiation coefficients are constant. This time invariant assumption, which is necessary for simplified PRF calculations, also influences the conductive heat gain split calculations as formulated in Equation 1.

METHODOLOGY

The most recent version of the RTSM is codified in the ASHRAE Loads Toolkit (Pedersen et al. 2001). The objective of this investigation is to experimentally demonstrate the reliability of the RTSM as a simplified cooling load calculation

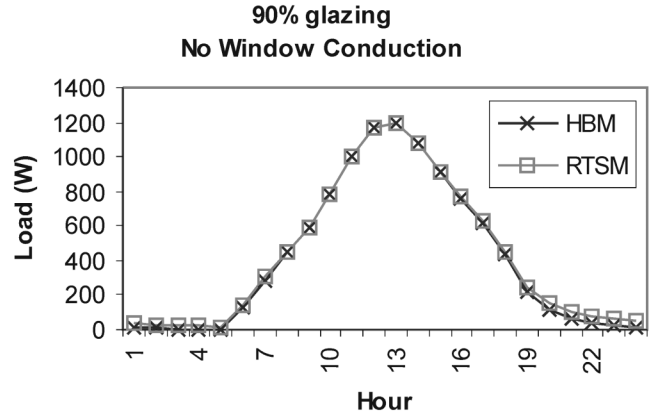


Figure 2 RTSM modified to correct errors.

procedure. This is accomplished by testing the extreme case of the solar dominated zone. Although the heat gain splits experimentally measured for this zone would not normally be encountered in most buildings (the solar heat gain exceeded 65% of the total heat gain for the test buildings), these conditions were selected in order to bound the error associated with the RTSM procedure. For all zones with a smaller fraction of solar to total heat gain, the expected error due to the procedure is less, often significantly less, than reported in this paper.

Experimental Procedure

Two geometrically identical buildings—one thermally massive and one thermally lightweight—as described in a companion paper (Eldridge et al. 2003), were constructed in an open field in Stillwater, Oklahoma. The first floor of each building consists of a mechanical/control room that provides conditioned air to the test cell located directly above, as shown Figure 3. The control room air temperature is maintained at the same temperature as the test cell in order to minimize heat conduction through the floor.

Elliptical flow nozzles measure the volumetric flow rate in the air loop. The room inlet and outlet air temperatures are also measured using thermocouple grids located in the ducts. The cooling load can then be calculated using the following equation:

$$Q_{\theta} = \dot{m}_{\theta} c_p (T_{out,\theta} - T_{in,\theta}) \quad (3)$$

For each set of experiments, the two test cells were identically configured. Both test cells had the same interior room configuration, and the indoor temperatures were controlled to the same value for each test. Four interior room parameters were varied during the tests, as shown in Table 1. Each parameter was designed to test the performance of different aspects of the RTSM algorithm.

TABLE 1
Test Cell Configurations

Test	Base	Ceiling	Carpet	Blinds	Mass	Office
Suspended Ceiling: 2 ft × 4 ft lay-in ceiling below bar joists	No	Yes	No	No	No	Yes
White Venetian Blinds	No	No	No	Yes (45° slats)	No	Yes (Horizontal slats)
Carpet with 0.25 in. pad	No	No	Yes	No	Yes	Yes
Thermal Mass: office furniture including desks, tables, chairs, and bookshelves filled with books	No	No	No	No	Yes	Yes

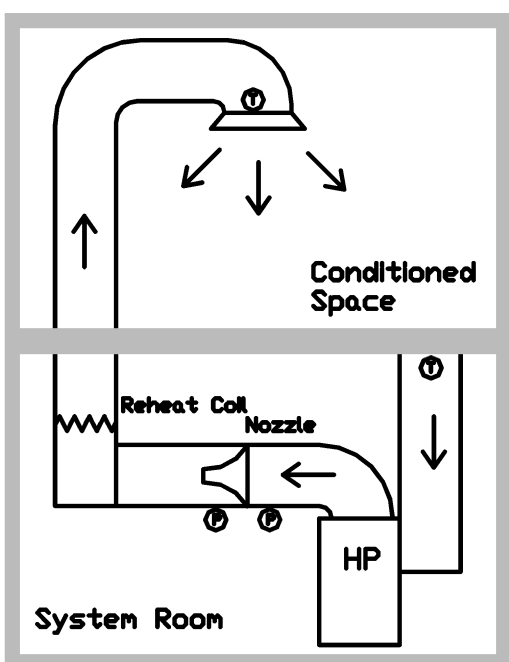


Figure 3 Terminal reheat system used in the RTSM validation (not to scale).

The experiments were designed to minimize internal and infiltration heat gains. Consequently, the cooling load was generated entirely by solar and conduction gains. Test conditions were maintained for more than 24 consecutive hours prior to data collection in order to allow the space to reach a steady-periodic state. Hourly cooling loads were measured and compared to cooling loads predicted by the RTSM under the same conditions.

Model Development

The measured cooling loads were compared to cooling loads predicted by two RTSM cooling load models—the basic RTSM model and the modified RTSM model. Both models

were based on the ASHRAE Loads Toolkit (Pedersen 2001) algorithms.

Basic Model Validation. The basic model uses both Toolkit algorithms and measured input data in the calculation. The measured input parameters are: outdoor and indoor temperatures, ground surface temperature, infiltration, globe horizontal solar radiation, wind speed, wind direction, system airflow rate, and surface shortwave absorptances. This validation procedure minimizes the error due to incorrectly estimated inputs and provides an estimate of the ability of the RTSM to accurately predict cooling loads.

Modifications to the Toolkit algorithms were made in order to use the measured input parameters in the test. Table 2 summarizes the use of input parameters and the associated heat transfer models used in the RTSM. The measured parameters are the hourly input parameters in the associated Toolkit modules. In addition, in order to agree with the RTSM assumptions, average measured indoor temperatures are used in the calculation procedure. The PRFs and RTFs are generated using average outside and inside surface film coefficients.

The inside heat balance parameters have a major impact on the resulting cooling load. This is particularly true of the inside convection because it results in a direct contribution to the cooling load. Table 3 compares the ASHRAE natural convection coefficients to the ceiling-diffuser convection coefficients (Fisher and Pedersen 1997) used in this validation. Note that the convection coefficients in the ASHRAE model are based on “reduced convection” at the ceiling due to thermal stratification. As a result, the ASHRAE model underestimates the inside convection for the high ventilation rates present in the test buildings.

Modified Model Validation. The modified model uses the same Toolkit algorithms and input data used by the basic model. In addition, the modified model accounts for shortwave radiation heat loss through glazed surfaces. The shortwave radiation heat loss is due to shortwave radiation from internal gains, diffuse solar radiation, and the portions of transmitted solar radiation heat gains that are reflected from the floor and transmitted out of the space through the windows.

TABLE 2
Summary of Input Parameters and Heat Transfer Models for the RTSM Validation

Input Data / Heat Transfer Models	Methods
Indoor air temperature	Measured data
Sol-air temperature	<ul style="list-style-type: none"> • Detailed sol-air temperature model • Measured outdoor air temperature • Measured shortwave absorptances: 0.9 for roofs, 0.7 for heavy building, and 0.6 for light building exterior surfaces • Measured ground surface temperature • BLAST sky temperature model • ASHRAE surface view factor model
Sky (solar) radiation	Modified ASHRAE clear sky model with measured global horizontal solar radiation
Ground surface temperature	Measured data
Conduction	State-space conduction (Seem 1987)
Surface convection coefficients	<ul style="list-style-type: none"> • Outside: MoWitt model with hourly measured wind speed and direction • Inside: Fisher and Pedersen (1997) model
Surface radiation coefficients	<ul style="list-style-type: none"> • Outside: Walton (1983) model • Inside: Walton (1980) model
Infiltration	BLAST model with 0.25 ACH hourly measured values
Conductive heat gain splits	Detailed splits, Equation 1

TABLE 3
Comparison of Interior Convection Models

Convection Coefficients	ASHRAE	Fisher and Pedersen (1997)*
Ceiling	1.250	20.497
Wall	4.679	7.294
Floor	4.370	5.380

* Based on 19.5 ACH

The calculation procedure of the modified RTSM includes the following algorithm to determine the amount of shortwave radiation heat gain that is transmitted out of the building space through the windows. First, the total diffuse shortwave heat gain is calculated as

$$Q_{sw,\theta} = Q_{r,beam,\theta} + Q_{diffuse,\theta} + Q_{sw,int,\theta}, \quad (4)$$

where $Q_{r,beam}$ is the portion of the beam radiation that is reflected diffusely from the floor, $Q_{diffuse}$ is the diffuse solar radiation transmitted into the building space, and $Q_{sw,int}$ is the shortwave radiation from internal loads.

By assuming that the beam solar radiation is distributed only on the floor, while the diffuse solar radiation is distributed uniformly on each interior surface, $Q_{r,beam}$ can be calculated as follows:

$$Q_{r,beam,\theta} = s_{floor} \rho_{t,floor} Q_{beam,\theta}, \quad (5)$$

where s_{floor} is the solar fraction and $\rho_{t,floor}$ is the shortwave reflectance of the floor. Note that the values of beam radiation Q_{beam} and diffuse radiation $Q_{diffuse}$ are available in the standard RTSM calculation procedures. The total diffuse short-

wave radiation heat loss through the windows is related to the total shortwave heat gain in the zone, as shown in Equation 6.

$$Q_{SW,loss,\theta} = Q_{sw,\theta} \sum_{k=0}^{\#windows} s_k \tau_{t,k} \quad (6)$$

where s is the solar fraction and τ_t is the transmittance of the windows. In the RTSM, the solar and radiant gains are operated on by RTFs to obtain cooling loads. In order to properly account for the loss of solar radiation that is reflected from interior surfaces and leaves the space through the windows, the shortwave radiation heat loss must be calculated and subtracted from the hourly total radiant heat gain before the radiant heat gain is processed by the RTFs.

RESULTS

Predicted Heat Gains

For a 40°C (104°F) design day outside dry-bulb and constant 25°C (77°F) inside air boundary temperatures, Table 4 shows the individual heat gain contribution to the total heat gain for the lightweight building with the base configuration.

TABLE 4
Typical Light Building Heat Gain Splits

Component Heat Gain	Q^*_{infil}	Q^*_{cond}	Q^*_{solar}	$Q^*_{internal}$
Heat Gain Fraction	0.65%	31.85%	67.50%	0.0%

The heat gain fractions were calculated from the following formulation:

$$Q^* = \frac{\sum_{\theta=1}^{24} Q_{\theta}}{\sum_{\theta=1}^{24} Q_{tot,\theta}} \quad (7)$$

where

Q^* = heat gain fraction

Q = component heat gain, W or Btu/h

Q_{tot} = total heat gain, W or Btu/h

The following component heat gains are shown in the table:

Q^*_{infil} = infiltration heat gain fraction

Q^*_{cond} = air-to-air conductive heat gain fraction

Q^*_{solar} = transmitted solar heat gain fraction

$Q^*_{internal}$ = internal heat gain fraction

For the test building, the cooling load is dominated by the solar heat gain with a significant contribution from the conductive heat gain. Infiltration is insignificant, and internal gains are nonexistent. Since the air-to-air conductive heat gain is calculated using the sol-air temperature and air-to-air PRFs, the conductive heat gain includes convection, longwave radiation, and surface incident solar radiation in addition to surface-to-surface conduction. As a result, the contribution of air-to-air conduction to the total heat gain is relatively high.

The heat gain splits shown in Table 4 represent extreme operating conditions, and the procedural error associated with these conditions is significant. Rees et al. (1998) calculated the deviation of the peak RTSM cooling load from the peak HBM cooling load for 1296 cases. Figure 4 shows the experimental test case data predicted by the modified RTSM (117-RP) superimposed on the Rees data (RP-942). As shown in the figure, the experimental test cases are well within the expected range of uncertainty for the RTSM even though they represent extreme operating conditions.

Figure 4 shows a deviation from the heat balance of less than 23% for all cases, even when the peak cooling load is relatively low. For cooling loads greater than 300 W/m² (95.13 Btu/h·ft²), the modified RTSM deviates from the HBM by less than 17%.

Modeling Thermal Mass Effect

The thermally massive test cell was constructed of 8 in. (20.32 cm), filled, heavyweight concrete blocks with a brick

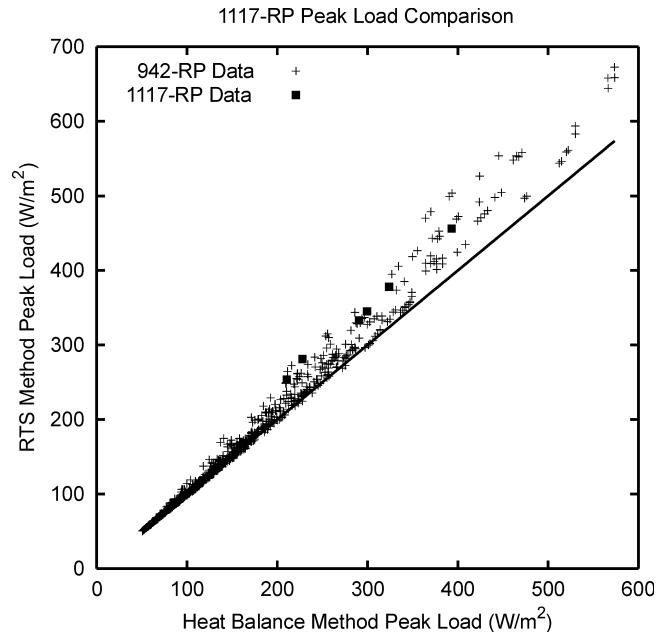


Figure 4 Comparison of RP-1117 results with Rees parametric study.

vener, a 5 in. (12.7 cm) concrete roof, and a 5 in. (12.7 cm) concrete floor. The lightweight test cell consisted of wood-framed walls with an exterior insulated finish system (EIFS) veneer, a built-up insulated roof, and a 3.5 in. (8.89 cm) concrete floor. Both test cells had large windows (50% glazing) on the south and west walls. The periodic response factors shown in Figure 5 illustrate the different thermal responses of the building elements.

The abrupt change of the wall and roof PRFs for the light building means that the thermal responses of these surfaces are faster than the heavy building wall and roof. Based on the surface response factors, one might expect the zone thermal response to be significantly different for the two buildings. However, the dominance of the solar heat gain ensures that the RTFs rather than the PRFs will largely determine the zone response. Figure 6 shows the radiant time factors for diffuse and beam solar radiation. The difference between diffuse RTF and beam RTF is due to different radiation distributions. The diffuse RTF assumes that radiation is distributed uniformly on all interior surfaces; the fast thermal response of the lightweight walls and roof causes the diffuse RTF to decrease faster. The beam RTF assumes that radiation is distributed

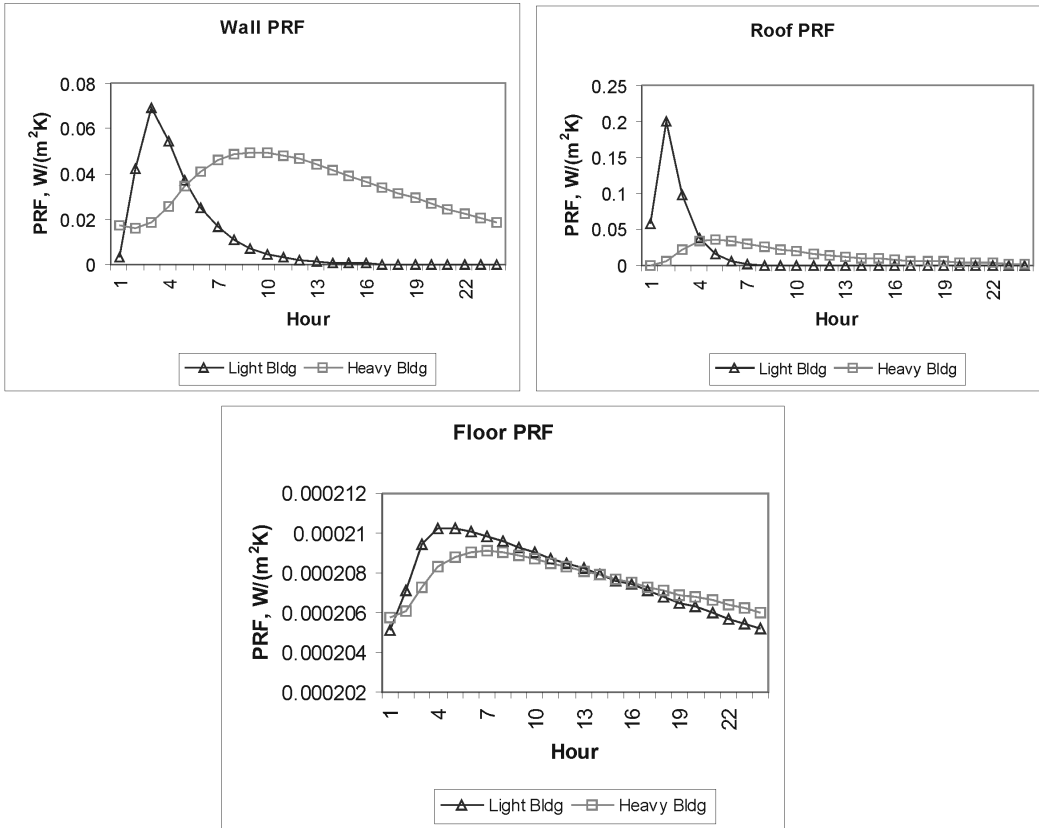


Figure 5 Periodic response factors for test buildings surfaces.

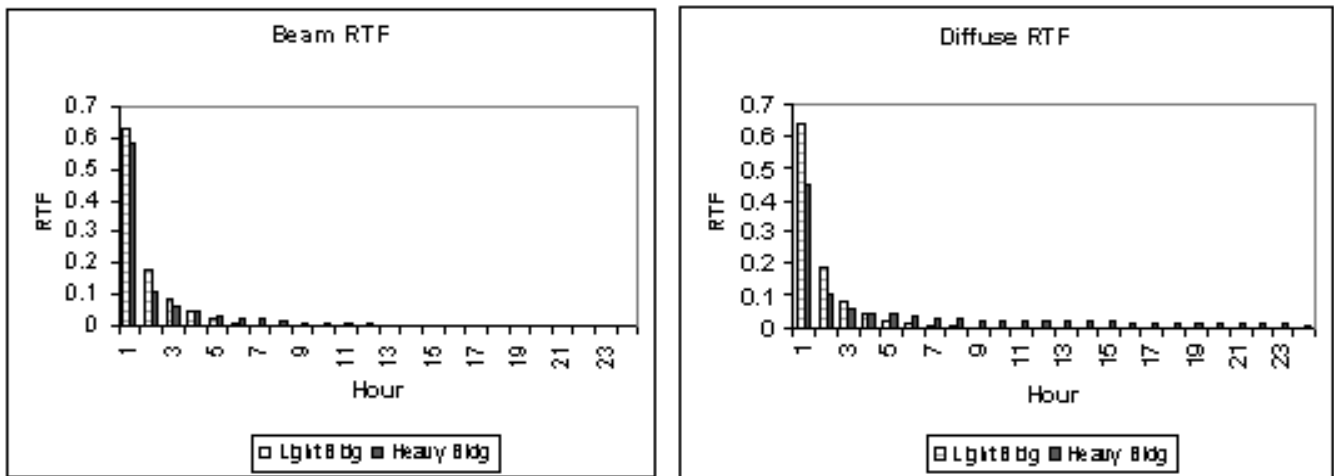


Figure 6 Radiant time factors for test buildings.

only on the floor, and since the building floor constructions are similar, the zone RTFs are also similar.

The overall effect of the building thermal mass is shown in Figure 7. The figure shows the measured cooling load for the two buildings under identical operating conditions. As shown by the “load” plot, the thermal mass of the heavy building damps the peak load by 25% but shows no discernible shift in the peak hour. The “fraction of peak load” plot shows the same cooling load profiles normalized as follows:

$$Q_N = \frac{Q_{est} - Q_{min,exp}}{Q_{max,exp} - Q_{min,exp}} \% \quad (8)$$

where Q_N is the normalized cooling load, Q_{est} is the estimated cooling load, and $Q_{min,exp}$ and $Q_{max,exp}$ are the minimum and maximum measured cooling loads, respectively. Presenting the measured data in this way shows that the thermal response times of the two buildings are very similar in spite of significant differences in the building thermal mass.

As reported in a companion paper (Chantrasrisalai et al. 2003), the HBM correctly predicts both the peak load reduction and the peak time. The HBM models were therefore used in a small parametric study to gain additional insight into the thermal response of the experimental buildings. As a result of this simulation study, the following conclusions are reached:

- The high percentage of glazing on the south and west walls (50% by outside surface area) effectively “short-circuits” the building thermal mass. Removing the windows in the simulation study results in a significant time shift.
- The peak time is relatively insensitive to the magnitude of interior convection coefficient. High convection coefficients associated with 19.5 ACH and natural convection coefficients for both high glazing and no glazing cases result in less than a 0.5 hour change in the peak hour.

Although the convection coefficient has little effect on the peak time, it has a significant effect on the magnitude of the peak load. This is illustrated in a companion paper (Chantrasrisalai et al. 2003), which shows that significant error can be introduced in the peak load calculation by not adjusting the convection coefficients to match the ventilative flow rate required to meet the hourly cooling load. For example, using the ASHRAE default (natural convection) correlations to model the heavyweight buildings (which required 20 ACH to meeting the cooling load) results in the HBM underpredicting the peak load by more than 20%.

Prediction of Peak Cooling Loads

Cooling load data for each of the test configurations were collected and compared with the RTSM predicted results as shown in Figure 8 and Figures 10 through 14. Each plot shows both measured and predicted hourly cooling loads, which are defined in the figures as follows:

- Measured—measured cooling load
- HBM—cooling load predicted by heat balance method with measured input data
- RTSM—cooling load predicted by the basic RTSM model
- RTSM-Modified—cooling load predicted by the modified RTSM model

All cooling loads are shown as a fraction of the measured load range. The actual load range (peak load and minimum load) used to calculate the fraction of full load is also shown in each figure. Showing the data as a fraction of measured load facilitates estimation of the peak load error associated with the RTSM and the HBM for each case. The peak error associated with each method can be read directly from the graphs.

Base Configuration. This test compares the measured cooling loads for an empty room with the RTSM predicted

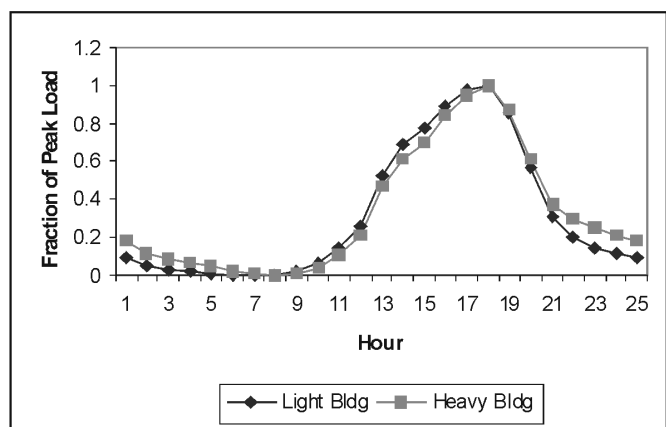
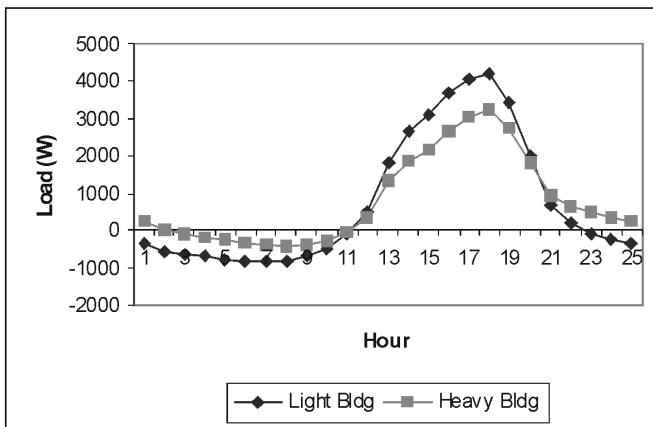


Figure 7 Thermal mass effects.

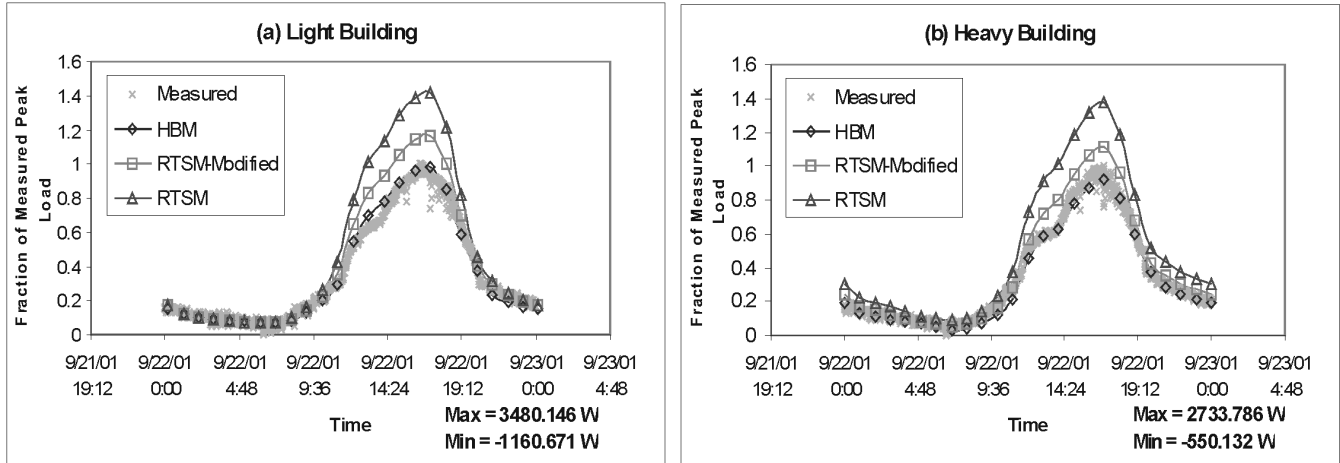


Figure 8 Base configuration.

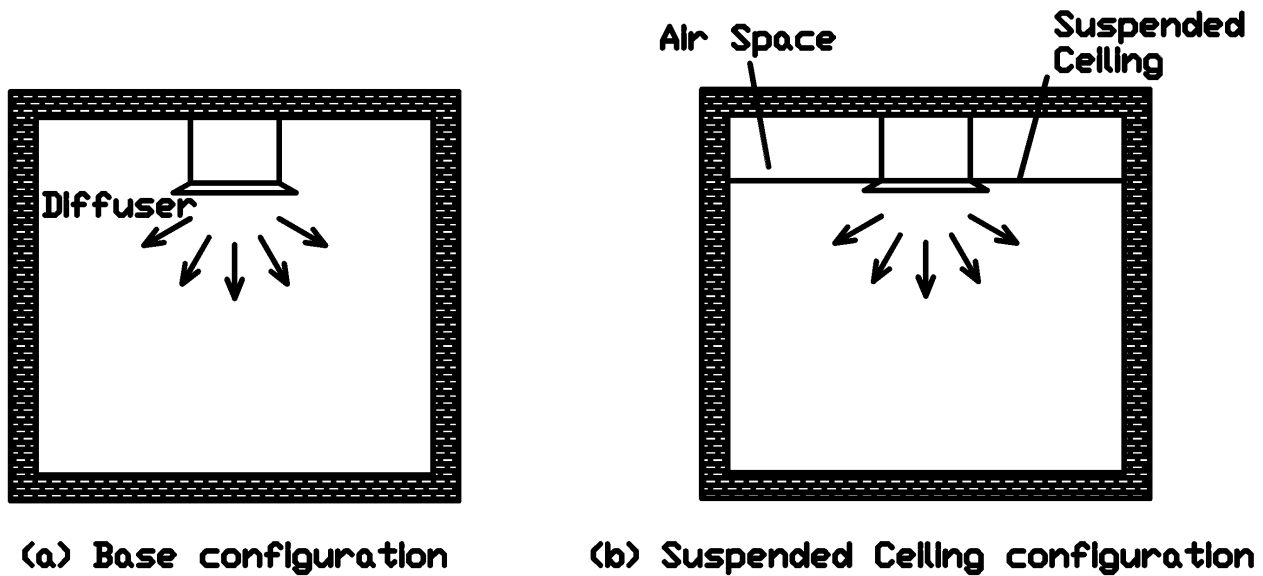


Figure 9 Ceiling diffuser configurations.

loads. The comparison is shown in Figure 8. Although most of the input uncertainties are eliminated in the basic model, the RTSM overpredicts the peak cooling load as expected for the solar-dominated experimental rooms. This is due to two uncorrected errors in the Toolkit RTSM, as discussed above. Although the conductive heat loss error was not corrected, the radiation correction was implemented. This correction reduces the peak load errors in both buildings by more than 50%, as shown by the RTSM-modified curves.

The damping effect of the thermally massive heavy building is also shown in Figure 8. The cooling load is shifted off

peak by the heavy building, resulting in a 25% reduction in the peak cooling load.

Suspended Ceiling Configuration. This test configuration required installation of suspended ceilings in the test cells, as shown in Figure 9. Note that the diffuser remained fixed at the same level for both the suspended ceiling and the base case configuration. The correlation used to obtain the ceiling convection coefficient was a better match for the suspended ceiling case than for the base case. That is, the correlations were developed for an attached radial ceiling jet (Fisher et al. 1997). As a result, the error in the cooling load predicted by the

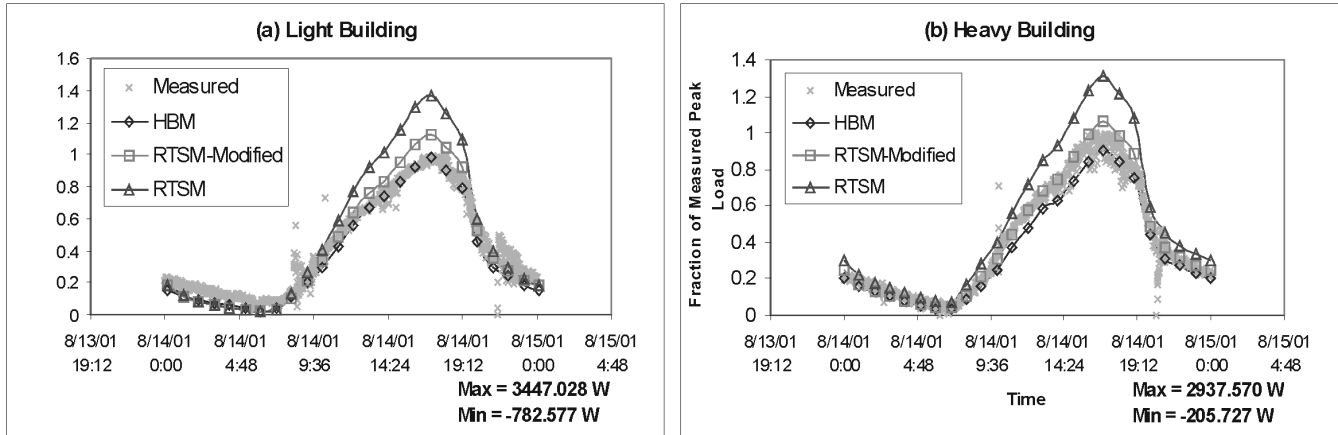


Figure 10 Suspended ceiling.

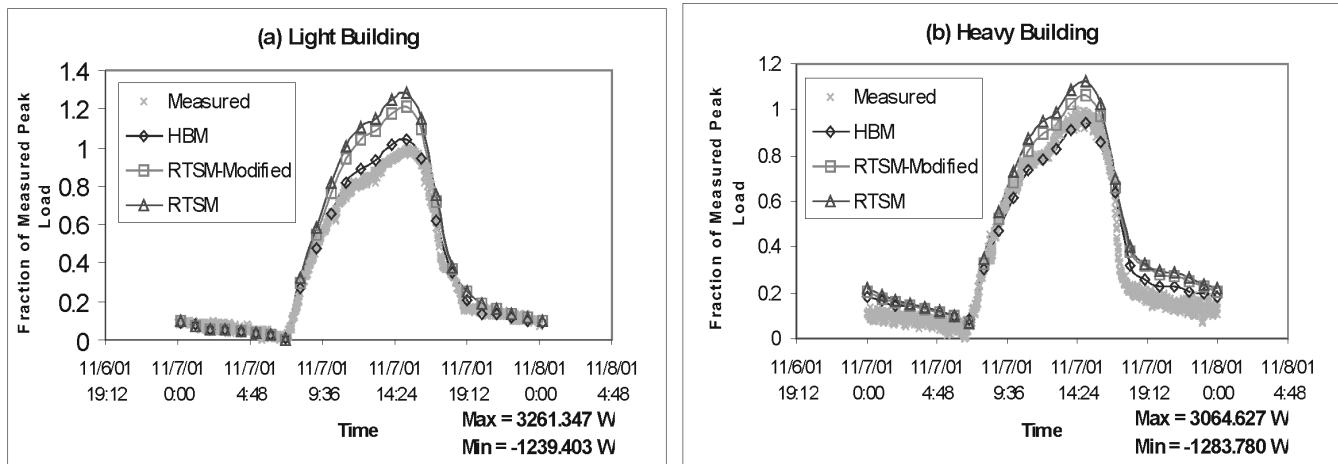


Figure 11 Office configuration.

RTSM was less for the suspended ceiling case, as shown in Figure 10. The basic trends, however, were the same, with the radiation loss correction significantly improving the results and the remaining peak errors about the same for the both buildings.

Mass Configuration. Thermal mass was added to the carpet configuration in the form of office furniture and books.

Office Configuration. Figure 11 shows cooling load comparisons for an office configuration that includes blinds, carpet, and thermal mass. Thermal mass was added to the carpet configuration in the form of office furniture and books. The blind slats are in a horizontal position, resulting in higher beam solar radiation heat gains compared to the blind configuration. The blinds may also influence the surface convection coefficients in this test. The thermal mass in the test cells alle-

viates the unaccounted for conduction error, and the suspended ceiling results in a better approximation of the interior convection coefficient at the ceiling level. The discrepancy between the RTSM and the HBM for this configuration is primarily due to the fact that a sophisticated blind model was implemented in the heat balance procedure in order to achieve good agreement with measured data, as discussed in the companion paper (Chantrasrisalai et al. 2003).

Summary of Results. Table 5 summarizes the peak errors predicted by the basic and modified RTSM models for all test cases. In order to improve the overall performance of the RTSM for these cases, the HBM must first be improved. The peak errors of the tests change depending on the uncertainties associated with the interior configurations.

The shortwave correction significantly improves the RTSM results for all test configurations. For the experimental

TABLE 5
Summary of Peak Load Errors Predicted by RTSM

RTSM Basic Model						
Test	Base	Ceiling	Blinds	Carpet	Mass	Office
Light Bldg	41.93%	36.98%	37.86%	44.45%	35.59%	28.08%
Heavy Bldg	37.36%	31.49%	19.4%	42.22%	NA	12.49%
RTSM Modified Model						
Test	Base	Ceiling	Blinds	Carpet	Mass	Office
Light Bldg	16.89%	12.66%	26.61%	29.83%	24.41%	21.05%
Heavy Bldg	11.14%	6.4%	8.65%	28.17%	NA	6.63%

NA = Not available

rooms, maximum deviation from the heat balance is 20% and maximum deviation from the measured data is 29%. As previously explained, this represents the maximum expected error for a zone with a transmitted solar heat gain contribution of 67.5% of the total heat gain. For typical applications, the error is expected to be much less.

Figure 12 shows the cooling load predicted by the RTSM and HBM for an office configuration with a 1.52 m × 1.52 m (5 ft × 5 ft) sized window on the west-facing wall. The window is a double-pane, low emissivity glass and is shaded at all times with a 45° venetian blind. The boundary conditions are 40°C (104°F) design day outside dry-bulb and constant 25°C (77°F) inside air temperatures. Internal heat gains were also considered in this simulation: two people are working in each build-

ing during office hours; two computers are used continuously and are in saver mode in the evening until the people come back the next morning; two 40 W lamps are on when the people are there. This configuration represents one of the low solar heat gain cases that would fall on the 45 degree line shown in Figure 4. For this case, the RTSM results are almost identical to the HBM results, as shown in Figure 12. The off-peak load difference is due to the constant film coefficients used in the RTSM. Table 6 summarizes the individual heat gain contribution to the total cooling load for the light building. Comparing these heat gains to the experimental heat gains (Table 4), shows that the air-to-air conductive heat gain dominates the thermal processes. Although the window area is smaller, the transmitted solar heat gain still contributes signif-

TABLE 6
Heat Gain Fractions for Typical Building Configurations

Component Heat Gain	Q^*_{infil}	Q^*_{cond}	Q^*_{solar}	$Q^*_{internal}$
Heat Gain Fraction	2.78%	55.81%	27.42%	13.99%

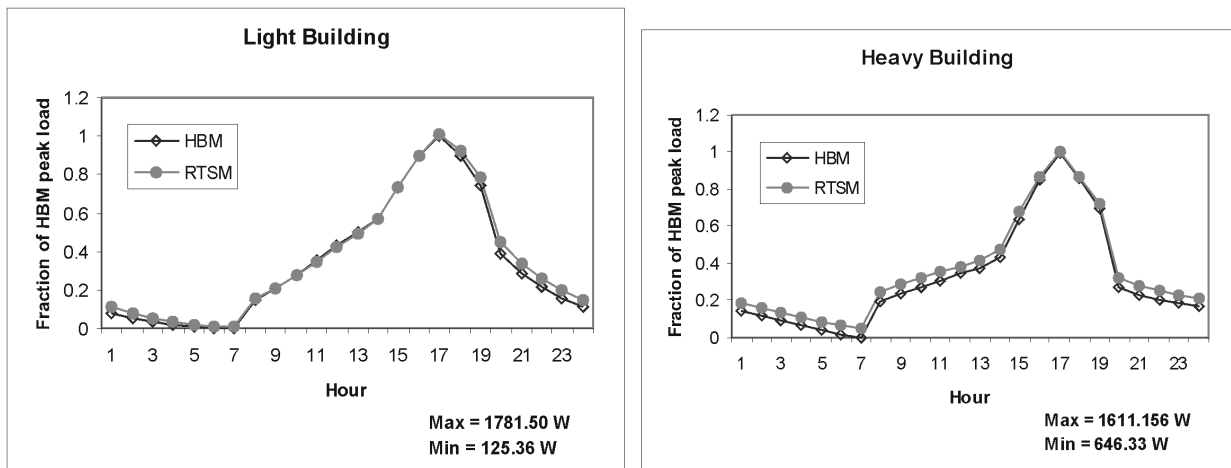


Figure 12 Simulations for typical building configurations.

icantly to the total cooling load. The internal heat gains are about 50% of the transmitted solar heat gains. The infiltration rate was not changed for the typical office simulation. Rees et al. (1998) provide a detailed discussion of the expected deviation of the RTSM from the HBM over the expected range of input parameters.

CONCLUSIONS AND RECOMMENDATIONS

The experimental results illustrate the utility of the RTSM, even for the extreme case of a conditioned sun space with no internal gains. The modified RTSM overpredicts the heat balance by less than 20% for all cases. This is quite reasonable for the heat gain split (67.5% solar) observed in the experiments. Simulation of a typical building configuration with internal heat gains and less transmitted solar radiation shows that the RTSM can be expected to match the HBM predicted peak cooling load for typical configurations.

The experimental results also highlight the importance of the reflected solar radiation correction for highly glazed zones. This correction can be easily implemented using information already available in the RTSM algorithms. It is recommended that the correction be included in the next version of the ASHRAE Loads Toolkit. Additional work to correct for the conduction losses from the zone is not recommended. The adiabatic zone assumption is an implicit simplification in the RTSM; derivation of additional correction factors unnecessarily complicates the method. Rather, future research should be aimed at improving the heat balance models and refining and cataloging model input parameters. Improvements in the HBM will be propagated to the RTSM and result in the improved accuracy of both methods. Implementation of adequate blind models in both procedures is of particular importance.

The research also illustrated the importance of choosing interior convective heat transfer coefficients on the basis of the ventilative flow rate. Using natural convection-based correlations for high ventilative flow rates can result in significant error in the calculated cooling load. Finally, the dominant effect of windows in determining the peak hour for the experimental buildings was illustrated by the research results. Fifty percent glazing on west and south walls completely eliminated any peak hour shift between the heavy and light buildings. Additional research is required to determine the effect of advanced glazing systems on the peak cooling load.

ACKNOWLEDGMENTS

This research project (RP-1117) was funded by ASHRAE and sponsored by ASHRAE TC 4.1. Tom Romine and Steve Bruning guided the project with a practiced eye and the invaluable

perspective gained by many years of experience in the field. Jeff Spitler and Simon Rees also contributed substantially to the research effort.

REFERENCES

- Chantrasrisalai, C., D.E. Fisher, I.S. Iu, and D.S. Eldridge. 2003. Experimental validation of design cooling load procedures: The heat balance method. *ASHRAE Transactions* 109(2).
- Eldridge, D.S., D.E. Fisher, I.S. Iu, and C. Chantrasrisalai. 2003. Experimental validation of design cooling load procedures: Facility design. *ASHRAE Transactions* 109(02).
- Fisher, D.E., and C.O. Pedersen. 1997. Convective heat transfer in building energy and thermal load calculations. *ASHRAE Transactions* 103(2). Atlanta: American Society of Heating, Refrigerating and Air-Conditioning Engineers, Inc.
- McQuiston, F.C., J.D. Parker, and J.D. Spitler. 2000. *Heating, Ventilating, and Air Conditioning—Analysis and Design*, 4th ed. New York: John Wiley & Sons, Inc.
- Pedersen, C.O., D.E. Fisher, and R.J. Liesen. 1997. Development of a heat balance procedure for calculating cooling loads. *ASHRAE Transactions* 103(2): 459-468. Atlanta: American Society of Heating, Refrigerating and Air-Conditioning Engineers, Inc.
- Pedersen, C.O., D.E. Fisher, R.J. Liesen, and R.K. Strand. 2001. *A Toolkit for Building Load Calculations*. Atlanta: American Society of Heating, Refrigerating and Air-Conditioning Engineers, Inc.
- Rees, S.J., J.D. Spitler, and P. Haves. 1998. Quantitative comparison of North American and U.K. cooling load calculation procedures—Results. *ASHRAE Transactions* 104(2): 36-46. Atlanta: American Society of Heating, Refrigerating and Air-Conditioning Engineers, Inc.
- Seem, J.E. 1987. Modeling of heat transfer in buildings. Ph.D. thesis, University of Wisconsin-Madison.
- Spitler, J.D., D.E. Fisher, and C.O. Pedersen. 1997. The radiant time series cooling load calculation procedure. *ASHRAE Transactions* 103(2): 503-515. Atlanta: American Society of Heating, Refrigerating and Air-Conditioning Engineers, Inc.
- Walton, G.N. 1980. A new algorithm for radiant interchange in room loads calculations. *ASHRAE Transactions* 86(2): 190-208.
- Walton, G.N. 1983. *Thermal Analysis Research Program Reference Manual*. National Bureau of Standards. NBSSIR 83-2655.